ORGANIC LETTERS

2012
Vol. 14, No. 24
6326–6329

Planar Star-Shaped Organic Semiconductor with Fused Triphenylamine Core for Solution-Processed Small-Molecule Organic Solar Cells and Field-Effect Transistors

Sanghyun Paek,[†] Nara Cho,[†] Shinuk Cho,[‡] Jae Kwan Lee,*[,§] and Jaejung Ko*[,†]

Department of New Material Chemistry, Korea University, Chungnam, 330-700, Republic of Korea, Department of Physics and EHSRC, University of Ulsan, Ulsan, 680-749, Republic of Korea, and Department of Chemistry Education, Chosun University, Gwangju, 501-759, Republic of Korea

chemedujk@chosun.ac.kr; jko@korea.ac.kr

Received November 12, 2012

ABSTRACT

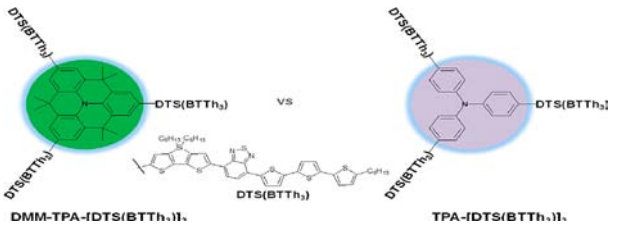

The symmetrical planar star-shaped organic semiconductor DMM-TPA-[DTS($BTTh_3$)]$_3$ with fused TPA core donor and three branch motifs, DTS($BTTh_3$), exhibited efficient *p*-type semiconducting performance in solution-processed SMOSCs and OFETs compared to the tilted star-shaped TPA-[DTS($BTTh_3$)]$_3$; a noteworthy PCE value of 4.16% was observed, with a hole mobility and on/off ratio of 7.6 $\times$ 10^{-3} cm^2 V^{-1} s^{-1} and 5 $\times$ 10^6, respectively.

Organic solar cells (OSCs) fabricated by versatile printing methods such as the doctor blade, inkjet, and roll-to-roll methods are inexpensive, lightweight, and highly solution-processable. Over the past few years, considerable effort has been focused on improving the OSC performance, with the aim of achieving a power conversion efficiency (PCE) of 10%. The following strategies have been adopted for this purpose: (1) development of photoactive materials such as π-conjugated semiconducting polymers and fullerenes, (2) use of functional layers for buffering, charge transport, optical spacing, etc., and (3) tuning the morphology of the photoactive film by postannealing, solvent drying, or using processing additives.[1,2] In particular, semiconducting polymers with new structures, affording PCEs above 8% in bulk-heterojunction (BHJ) OSCs fabricated using [6,6]-phenyl-$C_{61\ (or\ 71)}$-butyric acid methyl ester ($PC_{61\ (or\ 71)}BM$), have been developed; these polymers find potential applications in next-generation solar cells.[3] Over the past few years, considerable research has been focused on developing efficient small-molecule organic semiconductors to improve the performance of solution-processed small-molecule OSCs (SMOSCs), with the near-term goal of achieving a PCE comparable to that of polymer

[†] Korea University.
[‡] University of Ulsan.
[§] Chosun University.

(1) Demeter, D.; Rousseau, T.; Leriche, P.; Cauchy, T.; Po, R.; Roncali, J. *Adv. Funct. Mater.* **2011**, *21*, 4379–4387.
(2) Walker, B.; Kim, C.; Nguyen, T.-Q. *Chem. Mater.* **2011**, *23*, 470–482.
(3) Green, M. A.; Emery, K.; Hishikawa, Y.; Warta, W.; Dunlop, E. D. *Prog. Photovoltaics* **2011**, *19*, 565–572.
(4) Roquet, S.; Cravino, A.; Leriche, P.; Alévêque, O.; Frère, P.; Roncali, J. *J. Am. Chem. Soc.* **2006**, *128*, 3459–3466.
(5) Cravino, A.; Leriche, P.; Aleveque, O.; Roquet, S.; Roncali, J. *Adv. Mater.* **2006**, *18*, 3033–3037.
(6) Tamayo, A. B.; Dang, X. D.; Walker, B.; Seo, J.; Kent, T.; Nguyen, T. Q. *Appl. Phys. Lett.* **2009**, *94*, 103301–1–3.

10.1021/ol303045p
Published on Web 12/10/2012

solar cells (PSCs).[4−8] Small-molecule organic semiconductors are more attractive than polymer-based ones for mass production because the latter suffer from poor reproducibility of the weight-average molecular weight and polydispersity index and are difficult to purify.

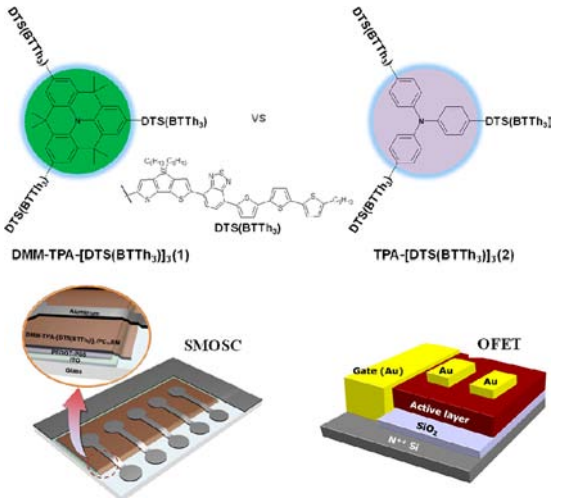

Figure 1. Molecular structure of **DMM-TPA-[DTS(BTTh$_3$)]$_3$** (**1**) and **TPA-[DTS(BTTh$_3$)]$_3$** (**2**) and device architectures of solution-processed small molecule organic solar cell and organic field-effect transistor.

A recent breakthrough in this regard has been reported by Sun et al., who successfully achieved PCEs exceeding 6% by using SMOSCs, thus making solution-processed SMOSCs strong competitors to PSCs.[9] Shang et al. have recently reported new symmetrical star-shaped acceptor−donor−acceptor (A−D−A) frameworks comprising a triphenylamine (TPA) core and various acceptors.[10] Thus inspired, we attempted to develop organic semiconductors with unique structures for use in solution-processed SMOSCs. The TPA unit does play important roles as electron donor and hole transport mediator, but it has a structure tilted between three aromatic benzene rings on a nitrogen atom that should be a crucial obstacle to intermolecular packing structure for efficient charge-transport in bulk-heterojunction (BHJ) system.

In this study, we synthesized a symmetrical planar star-shaped A−D−A organic semiconductor: tris[[4-[3,3′-dihexylsilylene-2,2′-bithiophene]-7-[5″-*n*-hexyl-(2,2′;5′,2″-terthiophene)-5-yl]benzo[*c*][1,2,5] thiadiazole]-2,6,10-yl]-4,4,8,8,12,12-hexamethyl-4*H*,8*H*,12*H*-benzo[1,9]quinolizino-[3,4,5,6,7]acridine (**DMM-TPA-[DTS(BTTh$_3$)]$_3$**, **1**) which has a TPA core (donor) and three branched motifs, DTS-(BTTh$_3$), comprising dithieno(3,2-b;2′,3′-d)silole (DTS), benzothiadiazole (BT), and hexylterthiophene units. SMOSCs and organic field-effect transistors (OFETs) based on this efficient *p*-type semiconductor exhibited a PCE and hole mobility of 4.16% and 7.6×10^{-3} cm^2 V^{-1} s^{-1}, respectively, with an on/off ratio of 5×10^6. We also compared the characteristics of this molecule with those of the tilted star-shaped tris[4-[3,3′-dihexylsilylene-2,2′-bithiophene]-7-[5″-*n*-hexyl-(2,2′;5′,2″-terthiophene)-5-yl]benzo[*c*][1,2,5]thiadiazole]-*p*-phenylene]amine (**TPA-[DTS(BTTh$_3$)]$_3$**, **2**) (Figure 1).

The synthetic methods are outlined in Scheme S1 (Supporting Information). Compounds **i**, **ii**, and **v** were synthesized according to the procedure reported previously.[11,12] Stille coupling reactions of **i** and **ii** with Pd(PPh$_3$)$_4$ as the catalyst in anhydrous toluene readily afforded **iii**. The DTS unit showed a smaller bandgap than did bithiophene, which is bridged by an sp^3 carbon, because of the low-lying LUMO and the greater stabilization of the HOMO. In addition, since the synthesized DTS(BTTh$_3$) has a motif similar to that of the highly efficient symmetrical A−D−A organic semiconductor, DTS-(PTTh$_2$)$_2$, which comprises a DTS donor and two [1,2,5]-thiadiazolo[3.4-*c*]pyridine (PT) acceptors end-capped with hexylbithiophene (reported recently by Sun et al.),[9] it might show broad absorption and good hole mobility.

Next, we introduced the planar TPA-bridged dimethylmethylene (DMM). The benzene rings in TPA have ∼35° of tilted angle on a nitrogen atom, while the tilt angle in DMM−TPA was much smaller because of the DMM bridge between the benzene rings. Moreover, the radical cation of DMM−TPA had a nearly planar structure. Thus, we supposed that the DMM−TPA core can facilitate intermolecular packing and increase the lifetime of the charge-separated state in the BHJ system more efficiently than does TPA. For bridging with DTS(BTTh$_3$), **v** was synthesized through modification of DMM−TPA by NBS according to a literature procedure.[10] Then, the organotin complex (**vii**) of DMM−-TPA was conducted with the **v** using *n*-BuLi and trimethyltin chloride. Finally, **1** could be successfully synthesized via Stille cross coupling with **vii** using Pd(PPh$_3$)$_4$ in anhydrous toluene. Compound **2** was also prepared from the bromo-TPA using the above-mentioned synthetic method. The chemical structures of **1** and **2** were verified by ^{1}H NMR, ^{13}C NMR, and MALDI-TOF mass analysis. Both these materials showed good solubility in common organic solvents such as methylene chloride, chloroform, chlorobenzene, and toluene.

Figure 2 shows UV−vis absorption spectra of **1** and **2** in chlorobenzene solution, in pristine thin film, and **1**/PC$_{71}$BM and **2**/PC$_{71}$BM BHJ films (1:4); the corresponding optical properties are summarized in Table S1 (Supporting Information) The $\pi-\pi^*$ transition and ICT transition bands of the planar star-shaped **1** showed a slight redshift as compared to those of the tilted star-shaped **2**, and

(7) Ma, C. Q.; Fonrodona, M.; Schikora, M. C.; Wienk, M. M.; Janssen, R. A. J.; Bauele, P. *Adv. Funct. Mater.* **2008**, *18*, 3323–3331.
(8) Ooi, Z. E.; Tam, T. L.; Shin, R. Y. C.; Chen, Z. K.; Kietzke, T.; Sellinger, A.; Baumgarten, M.; Mullen, K.; Mello, J. C. *J. Mater. Chem.* **2008**, *18*, 4619–4622.
(9) Sun, Y.; Welch, G. C.; Leong, W. L.; Takacs, C. J.; Bazan, G. C.; Heeger, A. *J. Nat. Mater.* **2012**, *11*, 44–48.
(10) Shang, H.; Fan, H.; Liu, Y.; Hu, W.; Li, Y.; Zhan, X. *Adv. Mater.* **2011**, *23*, 1554–1557.
(11) Beaujuge, P. M.; Pisula, W.; Tsao, H. N.; Ellinger, S.; Müllen, K.; Reynolds, J. R. *J. Am. Chem. Soc.* **2009**, *131*, 7514–7515.
(12) Do, K.; Kim, D.; Cho, N.; Paek, S.; Song, K.; Ko *J. Org. Lett.* **2012**, *14*, 222–225.

the molar absorptivity, too, was higher in the case of the former. In the thin-film state, the absorption bands of both **1** and **2** showed a redshift of ~40 nm relative to those in solution, and broader spectral peaks were observed because of intermolecular $\pi-\pi$ packing interactions. These results indicated that the planar structure of **1** results in higher molar absorptivity because of efficient ICT and $\pi-\pi^*$ transitions and facilitates intermolecular $\pi-\pi$ packing interactions more efficiently than does the tilted star-shaped structure of **2**, in solution and in the solid state.

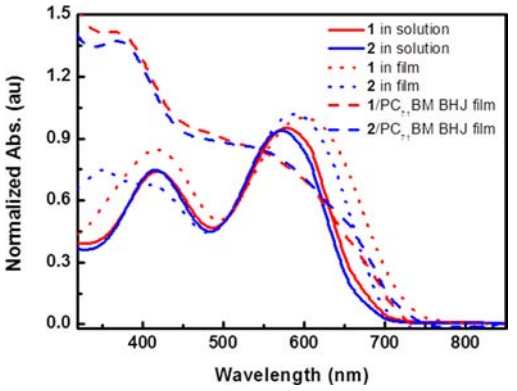

Figure 2. UV−vis absorption spectra of **1** (red) and **2** (blue) in chlorobenzene solution (solid line) and in pristine film (dotted line) and **1**/$PC_{71}BM$ BHJ (1:4) and **2**/$PC_{71}BM$ BHJ (1:4) films (dashed line).

From the cyclic voltammograms of **1** and **2** in Figure S1 and Table S1 (Supporting Information), the calculated HOMO/LUMO levels of **1** and **2** were 4.941/3.663 and 4.993/3.525 eV, respectively. These results indicated that the planar structure of TPA slightly increases the HOMO level as compared to that of the pristine TPA counterpart, leading to a slight decrease in V_{oc} of the BHJ devices fabricated using active layers with PCBM.[13]

To investigate the potential applicability of the two new compounds in plastic electronics, OFETs were fabricated in top-contact geometry. Figure 3a shows the transfer characteristics of the FET devices based on **1** and **2**. All the FETs were operated in accumulation mode; the applied source-drain bias (V_{ds}) during the transfer characteristic measurements was −60 V. The measured transport data were typical of *p*-channel OFETs: the devices were turned on under negative gate bias. The transfer characteristics data in Figure 3a indicated that the source-drain current (I_{ds}) is higher in the FET based on **1**. Higher FET performance was also evident from the output characteristics, as shown in Figure S2 (Supporting Information). The saturated hole mobilities of **1** and **2** were calculated using the saturation current equation: $I_{ds} = (WC_i/2L)\mu(V_{gs} - V_T)^2$, where W (= 50 μm) is the channel width; L (= 3000 μm), the channel length of the devices; C_i (= 15 nF/cm^2), the capacitance of the SiO_2 dielectric; and V_T, the threshold voltage. Linear plots of $I_{ds}^{1/2}$ vs V_{gs}, deduced from I_{ds} vs V_{gs} measurements (Figure S2a and S2b, Supporting Information), yielded a hole mobility of 7.6×10^{-3} cm^2/V·s and 2.2×10^{-3} cm^2/V·s for **1** and **2**, respectively. These FET results could be also corresponded to the hole mobilities of 2.53×10^{-5} cm^2/V·s (**1**) and 1.77×10^{-5} cm^2/V·s (**2**) evaluated using the space-charge limitation of current (SCLC) analysis (Figure S3, Supporting Information). We note that the planar structure can result in enhanced hole transport properties via efficient intermolecular $\pi-\pi$ packing interactions even in a BHJ system with $PC_{71}BM$.

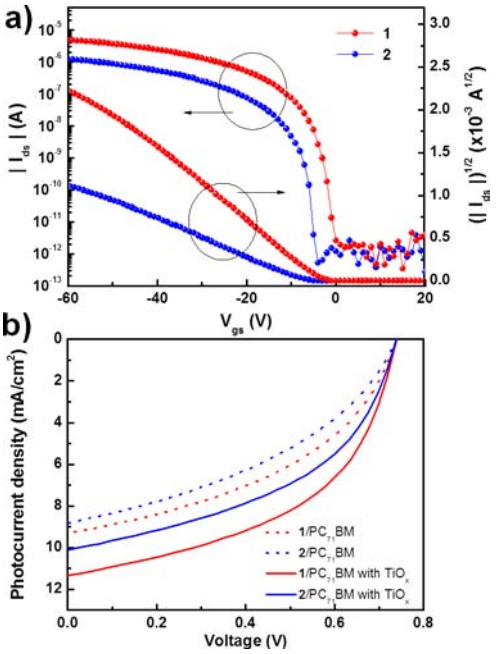

Figure 3. (a) Transfer characteristics of the FET devices based on **1** and **2**; (b) current (J)−voltage (V) curves of BHJ solar cells fabricated with **1**/$PC_{71}BM$ (red) or **2**/$PC_{71}BM$ (blue) under optimized processing conditions with (solid line)/without (dotted line) insertion of TiO_x layer.

These molecules were used for the fabrication of photovoltaic devices along with $PC_{71}BM$ BHJ films, which exhibited better performance with $PC_{71}BM$ than $PC_{61}BM$ due to good spectral response of $PC_{71}BM$ in visible region, and their performance was assessed.[14]

A study of more than 200 solar cells revealed that the most efficient photovoltaic cells were obtained from the BHJ system based on **1** or **2** with $PC_{71}BM$, which were optimized at a ratio of 1:4. The optimum thicknesses of the **1**/$PC_{71}BM$ and **2**/$PC_{71}BM$ BHJ films cast on a PEDOT:PSS layer were approximately 90 and 92 nm, respectively. Figure 2b shows the $J-V$ curves under AM 1.5 irradiation (100 mW/cm^2) and the IPCE spectra of the organic semiconductor/$PC_{71}BM$ BHJ solar cells fabricated under

(13) Scharber, M. C.; Muhlbacher, D.; Koppe, M.; Denk, P.; Waldauf, C.; Heeger, A. J.; Brabec, C. *J. Adv. Mater.* **2006**, *18*, 789–794.

(14) Lee, J. K.; Ma, W. L.; Brabec, C. J.; Yuen, J.; Moo, J. S.; Kim, J. Y.; Lee, K.; Bazan, G. C.; Heeger, A. J. *J. Am. Chem. Soc.* **2008**, *130*, 3619–3623.

optimized processing conditions with and without TiO_x, which can effectively act as an optical spacer and buffer layer,[15] between the photoactive layer and the Al electrode. The corresponding values are summarized in Table 1.

Table 1. Photovoltaic Performances of the Devices Fabricated with Star-Shaped Organic Semiconductors (**1** or **2**)/$PC_{71}BM$ BHJ Film[a]

materials	TiO_x insertion	J_{sc} (mAcm^{-2})	V_{oc} (V)	FF	η (%) max/avg
1	X	9.30	0.74	0.44	3.02/2.90
1	O	11.34	0.74	0.50	4.16/4.10
2	X	8.83	0.74	0.40	2.62/2.58
2	O	10.12	0.74	0.48	3.49/3.23

[a] The optimized BHJ films were spin-cast at 3000 rpm for 60 s. The photovoltaic characteristics were performed under simulated 100 mW/cm^2 AM 1.5G illumination. The light intensity used calibrated standard silicon solar cells with a proactive window made from KG5 filter glass traced to the National Renewable Energy Laboratory (NREL). The masked active area of the device is 4 mm^2.

The IPCE spectra of these devices show curves well-matched with their optical absorptions, resulting in close correlation with the photocurrents in the *J-V* curves (Figure S4, Supporting Information). As shown in Figure 3b and Table 1, the PCE, short-circuit current density (J_{sc}), fill factor (*FF*), and V_{oc} of the device fabricated conventionally from **1**/$PC_{71}BM$ were 3.02%, 9.30 mA/cm^2, 0.44, and 0.74 V, respectively. On the other hand, the device fabricated with **2**/$PC_{71}BM$ had PCE, J_{sc}, *FF*, and V_{oc} values of 2.62%, 8.83 mA/cm^2, 0.40, and 0.74 V, respectively.

The relatively higher J_{sc} and *FF* of **1** could be attributed to the better hole mobility resulting from the efficient intermolecular $\pi-\pi$ packing interactions, which in turn were facilitated by the planar skeleton of **1**. Moreover, the devices fabricated using **1**/$PC_{71}BM$ film with a TiO_x layer showed the best PCE of 4.16%, with J_{sc} = 11.34 mA·cm^{-2}, *FF* = 0.50, and V_{oc} = 0.74 V; thus, the performance was enhanced by ~38% as compared to that of the films without the TiO_x layer. The SMOSCs fabricated with **1**/$PC_{71}BM$ and **2**/$PC_{71}BM$ BHJ films showed significantly increased photocurrents (~20% and ~15% increase, respectively) and a slightly enhanced *FF* after insertion of the TiO_x layer. This was because the TiO_x layer allowed for increased light absorption and better contact between the active layer and the metal electrode in the device.[16]

In conclusion, we have synthesized a symmetrical planar star-shaped organic semiconductor, **DMM-TPA-[DTS-(BTTh$_3$)]$_3$**, and demonstrated its use as an efficient *p*-type organic semiconductor in solution-processed SMOSCs and OFETs. A high PCE of 4.16%, with a hole mobility of 7.6×10^{-3} cm^2 V^{-1} s^{-1} and on/off ratio of 5×10^6, were observed, indicating that the planar semiconductor showed better performance than did a similar molecule, (**TPA-[DTS(BTTh$_3$)]$_3$**, with a tilted star-shaped structure. The superior performance of the planar molecule probably resulted from the efficient intermolecular $\pi-\pi$ packing interactions and the consequent enhanced hole mobility. The findings of our study can be an important guide for the development of novel materials for use in efficient solution-processed SMOSCs and OFETs.

Acknowledgment. This research was supported by the World Class University program funded by the Ministry of Education, Science and Technology through the National Research Foundation of Korea (R31-2011-000-10035-0), a New & Renewable Energy of the Korea Institute of Energy Technology Evaluation ad Planning (KETEP) grant funded by the Korea government Ministry of Knowledge Economy (no. 20103060010020), and the Priority Research Centers Program (2009-0093818) through the NRF of Korea funded by the MEST.

Supporting Information Available. Characterization of synthetic materials, CV, SCLC, calculation of energy level, and AFM image of BHJ films. This material is available free of charge via the Internet at http://pubs.acs.org.

The authors declare no competing financial interest.

(15) Lee, J. K.; Coates, N. E.; Cho, S.; Cho, N. S.; Moses, D.; Bazan, G. C.; Lee, K.; Heeger, A. *J. Appl. Phys. Lett.* **2008**, *92* (243308), 1–3.
(16) Lee, K.; Kim, J. Y.; Park, S. H.; Kim, S. H.; Cho, S.; Heeger, A. *J. Adv. Mater.* **2007**, *19*, 2445–2449.